nature

SUPPLEMENTARY INFORMATION

https://doi.org/10.1038/s41586-019-1376-z

In the format provided by the authors and unedited.

Apidima Cave fossils provide earliest evidence of *Homo sapiens* in Eurasia

Katerina Harvati[1,2,3]*, Carolin Röding[1], Abel M. Bosman[1,2], Fotios A. Karakostis[1], Rainer Grün[4], Chris Stringer[5], Panagiotis Karkanas[6], Nicholas C. Thompson[1,3], Vassilis Koutoulidis[7], Lia A. Moulopoulos[7], Vassilis G. Gorgoulis[8,9,10]* & Mirsini Kouloukoussa[3,8]

[1]Paleoanthropology, Senckenberg Centre for Human Evolution and Palaeoenvironment, Eberhard Karls University of Tübingen, Tübingen, Germany. [2]DFG Centre of Advanced Studies 'Words, Bones, Genes, Tools', Eberhard Karls University of Tübingen, Tübingen, Germany. [3]Museum of Anthropology, Medical School, National and Kapodistrian University of Athens, Athens, Greece. [4]Australian Research Centre for Human Evolution, Griffith University, Nathan, Queensland, Australia. [5]Centre for Human Evolution Research, Department of Earth Sciences, The Natural History Museum, London, UK. [6]Malcolm H. Wiener Laboratory for Archaeological Science, American School of Classical Studies at Athens, Athens, Greece. [7]First Department of Radiology, National and Kapodistrian University of Athens, Athens, Greece. [8]Department of Histology and Embryology, Medical School, National and Kapodistrian University of Athens, Athens, Greece. [9]Biomedical Research Foundation of the Academy of Athens, Athens, Greece. [10]Division of Cancer Sciences, Faculty of Biology, Medicine and Health, Manchester Academic Health Science Centre, Manchester Cancer Research Centre, NIHR Manchester Biomedical Research Centre,, University of Manchester, Manchester, UK. *e-mail: katerina.harvati@ifu.uni-tuebingen.de; vgorg@med.uoa.gr

Supplementary Information

1. Uranium-Series dating

We analyzed samples from the 'skull breccia', selected from fragments produced in the process of cleaning the specimens from the matrix, with the U-series method. These included human bone fragments (subsamples 3720A, B, Apidima 2, and subsamples 3754, 3755, Apidima 1) and four unidentified bone subsamples (3757A-C, 3758, see Supplementary Fig. 1). The Apidima 1 remains have shiny, somewhat translucent and seemingly mineralised surfaces, as had the subsamples 3757B and C. The fragments from Apidima 2 have matte, soft surfaces, as had subsamples 3757A and 3758. The analyses followed the procedures described in detail in [49]. All isotope ratios in this paper are activity ratios. U-series age results on bones are generally regarded as minimum age results. Thus, all individual age estimates reported here are apparent closed system ages. The initial $^{234}U/^{238}U$ ratio ($^{234}U/^{238}U_i$) can be used to identify whether the source for the uranium in a bone has remained the same or may have changed, or whether there are different U-sources involved for the various materials analyzed. The earlier analysis of a larger cranial fragment of Apidima 2 was carried out in 2010 and published in [5]. The detailed analyses are shown in Supplementary Table 1 and Supplementary Fig. 2.

The two matrix sections 3720A and B show generally low $^{234}U/^{238}U$ ratios in the range of 1.09 to 1.11 and finite ages of around 150 ka (using a Th correction with an elemental Th/U ratio of 4.25 [50], see Supplementary Fig. 2E). This points to a calcification event around this time. The initial average $^{234}U/^{238}U$ ratios of the two sections are closely similar around 1.18 to 1.19. There are no relationships between measured $^{234}U/^{238}U$ ratios and age or U-concentrations and age (Supplementary Fig. 2A, B), indicating that no partial leaching or secondary U-overprint has occurred.

For discussing the various U-migration effects in the skeletal material, it is beneficial to start with the bone samples 3757A-C and 3758. The matte samples 3757A and 3758 show age results around 150 to 160 ka (Supplementary Fig. 2C, D). Sample 3758 has relatively low $^{234}U/^{238}U$ ratios of around 1.14, with $^{234}U/^{238}U_i$ ratios of ~1.22. 3758 shows no relationships between age and $^{234}U/^{238}U$ ratios or U-concentration. Sample 3757A has a similarly low measured $^{234}U/^{238}U$ ratios (~1.14) with $^{234}U/^{238}U_i$ ratios of ~1.22. However, the range of the $^{234}U/^{238}U$ ratios and U-concentrations in the individual analysis spots are much wider than for 3758 (Supplementary Fig. 2C,D) and there are also trends between ages and measured $^{234}U/^{238}U$ ratios or U-concentrations. The ages become younger with lower $^{234}U/^{238}U$ ratios as well as lower U-concentrations. The U-source for any secondary U-uptake event after the calcification of the breccia at around 150 ka would be located in the matrix, which has lower $^{234}U/^{238}U$ ratios than the bones. In other words, overprints with U from the breccia will lead to lower ages and $^{234}U/^{238}U$ ratios. Secondly, sample 3757 has domains with calcitic fillings (Supplementary Fig. 1, on the left side of the specimen), which have lower U-concentrations. Analysis # 7 has by far the lowest U-concentrations, a lower than average $^{234}U/^{238}U$ ratio and the youngest age. The lower U-concentration is most likely the result of pores filled with secondary calcite containing uranium derived from the matrix.

The "shiny" samples 3757B and C have generally higher measured $^{234}U/^{238}U$ ratios than the previous two and significantly older ages. Sample 3757C has $^{234}U/^{238}U$ ratios of around 1.22, with $^{234}U/^{238}Ui$ of ~1.43. The apparent ages are around 240 ka. Analyses #1 and #2 show signs of leaching and #10 secondary U-overprint. However, the overprint seems to have taken place before the sample was embedded in the matrix, as this analysis points to an uranium source with a much higher $^{234}U/^{238}U$ ratio (~1.34) than that of the matrix. Excluding this value from the average has little effect, as the U-concentrations are low. Sample 3757B has $^{234}U/^{238}U$ ratios of around 1.20, with $^{234}U/^{238}Ui$ ratios of ~1.38. While there is nearly no relationship between age and measured $^{234}U/^{238}U$ ratio, there is a clear relationship between age and U-concentration (Supplementary Fig. 2D). This may be explained with secondary fillings, however, with $^{234}U/^{238}Ui$ ratios significantly higher than the matrix.

The bone samples show that samples of different ages and U-isotope signatures are present in the matrix. The "shiny" samples 3757B and C accumulated their U-signature in a different environment from the breccia, well before the matrix was solidified. The "matte" samples 3757A and 3758 may have accumulated their U from a similar source as the breccia, perhaps while the latter was still uncemented. Only sample, 3757A seems to have had any direct U-exchange with the matrix.

The results for Apidima 1 and 2 are strikingly different. The previously analyzed specimen from Apidima 2 [5] had all finite ages and no relationships between apparent age and U-concentration or measured $^{234}U/^{238}U$ ratio (Supplementary Fig. 2E,F). The average measured $^{234}U/^{238}U$ ratio is 1.16 with an average age of 172±11 and a $^{234}U/^{238}Ui$ of 1.27. The analyses of the bone in 3720A fall well into this range (Supplementary Fig. 2E,F).

In contrast, sample 3754 from Apidima 1 showed mostly leaching effects ($^{230}Th/^{238}U$ » $^{234}U/^{238}U$) and sample 3758 showed widely varying results. The U-concentrations in Apidima 1 are significantly lower than of Apidima 2 and most of the $^{234}U/^{238}U$ ratios are much higher (Supplementary Fig. 2E,F). The results derived from the analyses #7 to 24 show no relationship between age and Th/U ratio. The average $^{234}U/^{238}U$ ratio of this section is ~1.30 with an age of 211±16 ka and an $^{234}U/^{238}Ui$ of 1.54. Analyses #25 to 30 return much lower ages and also lower $^{234}U/^{238}U$ ratios, which indicates a secondary overprint from a U-source with a much lower $^{234}U/^{238}U$ ratio. Considering the randomness of the U-results (see analytical results for #21-23, Supplementary Table 1), the variability of analytical results within section #7-24 is likely due to U-micro-migration [51].

Supplementary Table 1: Detailed U-series results.

3720A	U (ppm)	Th (ppb)	U/Th	$^{230}Th/^{238}U$	$^{230}Th/^{238}U$ error	$^{234}U/^{238}U$	$^{234}U/^{238}U$ error	Age (ka)	Age error (ka)
1	7.20	4	1637	0.9148	0.0133	1.1237	0.0067	173.2	6.6
2	6.15	13	459	0.8863	0.0150	1.1250	0.0063	160.7	6.4
3	7.46	18	421	0.8451	0.0092	1.1266	0.0066	144.9	3.8
4	1.96	1201	1.64	0.7896	0.0185	1.0816	0.0182	139.0	8.4
5	1.66	1519	1.09	0.8126	0.0211	1.0727	0.0125	150.3	9.3
6	1.43	1615	0.89	0.8436	0.0255	1.0763	0.0330	161.6	17.1
7	1.83	1643	1.11	0.8007	0.0227	1.0688	0.0317	147.1	13.6
8	1.65	1674	0.99	0.8607	0.0228	1.0696	0.0278	172.2	16.7
9	4.48	20279	0.22	1.0866	0.0603	1.0734	0.0194	465.7	403.8
10	2.13	3754	0.57	0.8765	0.0233	1.0659	0.0201	181.9	16.0
11	5.16	984	5.24	0.8949	0.0199	1.1224	0.0064	165.1	8.6
AVERAGE VALUES									
	initial $^{234}U/^{238}U$	$^{234}U/^{238}U$i Error		$^{230}Th/^{238}U$	$^{230}Th/^{238}U$ error	$^{234}U/^{238}U$	$^{234}U/^{238}U$ error	Age (ka)	Age error (ka)
1-3	1.1958	0.0113		0.8813	0.0177	1.1251	0.0078	158.7	7.4
4-11, not 9	1.1405	0.0139		0.8525	0.0180	1.0894	0.0096	160.3	8.3
Th/U=4.25 correction	1.1824	0.0110		0.8572	0.0167	1.1189	0.0077	151.6	6.7

3720B	U (ppm)	Th (ppb)	U/Th	$^{230}Th/^{238}U$	$^{230}Th/^{238}U$ error	$^{234}U/^{238}U$	$^{234}U/^{238}U$ error	Age (ka)	Age error (ka)
1	0.48	486	0.99	0.8988	0.0337	1.0663	0.0259	193.9	24.8
2	0.80	1192	1.64	0.8208	0.0337	1.0580	0.0207	159.1	16.7
3	1.73	1292	1.45	0.8085	0.0245	1.0820	0.0149	145.7	10.2
4	0.97	961	0.75	0.7603	0.0259	1.0714	0.0252	132.0	11.0
5	0.58	386	0.60	0.9211	0.0315	1.0931	0.0225	191.0	21.1
6	5.48	919	14.23	0.8860	0.0247	1.1144	0.0107	164.6	11.1
7	3.79	722	4.13	0.8457	0.0162	1.1193	0.0150	147.3	7.4
8	1.70	1604	2.36	0.8371	0.0251	1.0802	0.0187	157.4	12.5
9	0.47	470	0.29	0.9049	0.0378	1.0724	0.0215	193.8	25.0
10	1.34	954	2.86	0.8604	0.0227	1.0780	0.0162	168.3	12.4
11	5.79	995	6.07	0.9295	0.0127	1.1540	0.0092	167.2	6.2
12	4.76	1694	4.78	0.8597	0.0204	1.1103	0.0131	155.5	9.1
13	1.32	1287	0.78	0.8681	0.0221	1.0824	0.0142	169.9	11.9
AVERAGE VALUES									
	initial $^{234}U/^{238}U$	$^{234}U/^{238}U$i Error		$^{230}Th/^{238}U$	$^{230}Th/^{238}U$ error	$^{234}U/^{238}U$	$^{234}U/^{238}U$ error	Age (ka)	Age error (ka)
1-13	1.1723	0.0117		0.8705	0.0177	1.1097	0.0085	160.0	7.8
Th/U=4.25 correction	1.1872	0.0122		0.8551	0.0174	1.1228	0.0086	149.6	6.9

3754	U (ppm)	Th (ppb)	U/Th	$^{230}Th/^{238}U$	$^{230}Th/^{238}U$ error	$^{234}U/^{238}U$	$^{234}U/^{238}U$ error	Age (ka)	Age error (ka)
1	2.29	2.9	789	1.0944	0.0500	1.2712	0.0326	187.9	25.0
2	2.34	2.3	1000	1.1707	0.0471	1.2425	0.0283	245.1	39.7
3	1.85	2.8	659	1.2487	0.0569	1.2982	0.0410	254.9	51.9
4	1.76	2.6	685	1.4573	0.0566	1.2909	0.0291	leaching	
5	1.83	2.8	656	1.4642	0.0482	1.3330	0.0378	580.9	593.3
6	1.69	3.6	475	1.6054	0.0615	1.3315	0.0331	leaching	
7	1.99	2.2	919	1.6106	0.0690	1.3283	0.0359	leaching	
8	1.84	4.2	437	1.6004	0.0588	1.3310	0.0337	leaching	
9	1.75	3.8	456	1.6577	0.0658	1.3585	0.0249	leaching	
10	1.98	2.7	736	1.7474	0.0458	1.4114	0.0252	leaching	
11	1.70	2.1	800	1.6777	0.0578	1.3428	0.0270	leaching	
12	2.04	4.0	505	1.8493	0.0585	1.3706	0.0287	leaching	
13	1.85	5.0	374	1.7861	0.0566	1.3814	0.0269	leaching	
14	1.29	29.4	44	1.7660	0.0649	1.3676	0.0348	leaching	
15	1.16	19.6	59	1.5507	0.0772	1.3526	0.0306	leaching	
16	1.44	5.9	244	1.7192	0.0644	1.3826	0.0307	leaching	
17	0.87	8.0	109	1.6038	0.0862	1.3518	0.0433	leaching	
18	0.78	6.9	113	1.6023	0.1327	1.3775	0.0380	leaching	
19	1.44	6.6	216	1.6883	0.0621	1.3817	0.0244	leaching	
20	1.40	4.4	319	1.7484	0.0557	1.3748	0.0267	leaching	
21	0.54	8.3	65	1.6018	0.1572	1.3530	0.0545	leaching	
22	1.29	4.6	278	1.6875	0.0688	1.3913	0.0361	leaching	
23	1.34	4.7	285	1.5609	0.0680	1.3486	0.0250	leaching	
24	1.21	28.1	43	1.4721	0.0671	1.3333	0.0325	663.5	1231.1
25	1.03	15.2	68	0.5688	0.0555	1.1809	0.0369	70.2	10.0

3755	U (ppm)	Th (ppb)	U/Th	$^{230}Th/^{238}U$	$^{230}Th/^{238}U$ error	$^{234}U/^{238}U$	$^{234}U/^{238}U$ error	Age (ka)	Age error (ka)
1	1.69	189.6	9	1.1798	0.0493	1.2848	0.0309	221.7	32.5
2	1.34	122.8	11	1.4868	0.0835	1.3139	0.0295	0.0	0.0
3	1.16	147.0	8	1.3513	0.1079	1.3134	0.0302	333.5	147.5
4	0.37	112.9	3	0.4089	0.0746	1.1275	0.0499	48.7	11.5
5	0.95	41.9	23	1.7144	0.1096	1.3643	0.0414	0.0	0.0
6	1.11	231.1	5	1.4743	0.0952	1.3021	0.0314	0.0	0.0
7	1.06	78.2	14	1.1760	0.0857	1.2783	0.0393	223.6	53.3
8	1.71	5.6	305	1.3117	0.0894	1.2815	0.0292	334.8	131.9
9	1.46	10.1	144	1.3370	0.0670	1.3431	0.0299	281.6	62.4
10	1.88	7.0	270	1.1421	0.0667	1.3033	0.0411	194.2	33.5
11	0.34	15.0	22	1.1179	0.1501	1.3030	0.0639	184.5	63.9
12	0.91	9.3	97	1.2649	0.0862	1.3029	0.0328	262.6	69.9
13	1.57	55.2	28	1.1765	0.0572	1.2976	0.0324	212.8	33.3
14	2.07	12.3	169	1.1799	0.0607	1.2875	0.0282	220.2	36.4
15	1.45	5.0	287	1.2678	0.0775	1.3580	0.0486	225.8	48.6
16	1.90	6.3	301	1.1022	0.0478	1.2861	0.0312	185.0	22.9
17	1.45	7.2	201	1.1604	0.0865	1.2951	0.0376	206.3	45.0
18	1.61	15.3	105	1.2307	0.0548	1.3091	0.0228	235.3	35.7
19	1.47	19.1	77	1.2467	0.0715	1.3159	0.0291	240.3	47.9
20	1.60	3.5	458	1.0039	0.0631	1.2732	0.0377	154.4	22.6
21	1.53	3.7	416	1.1671	0.0983	1.3106	0.0267	201.9	45.8
22	1.15	2.7	424	1.3505	0.0752	1.3102	0.0346	337.8	116.7
23	2.51	8.0	314	0.9462	0.0504	1.2527	0.0202	142.4	15.6
24	1.95	5.8	338	1.1390	0.0870	1.2984	0.0361	195.1	40.7
25	3.56	9.6	370	0.7076	0.0344	1.2206	0.0155	91.4	7.0
26	2.61	13.9	188	0.6326	0.0568	1.2206	0.0203	77.5	10.1
27	1.77	58.6	30	0.3930	0.0700	1.1955	0.0240	43.0	9.3
28	1.90	64.9	29	0.3982	0.0690	1.1616	0.0328	45.3	9.8
29	2.04	59.7	34	0.3804	0.0664	1.1878	0.0230	41.6	8.8
30	1.47	66.3	22	0.1970	0.0300	1.1546	0.0207	20.3	3.4
AVERAGE VALUES									
	initial $^{234}U/^{238}U$	$^{234}U/^{238}Ui$ Error		$^{230}Th/^{238}U$	$^{230}Th/^{238}U$ error	$^{234}U/^{238}U$	$^{234}U/^{238}U$ error	Age (ka)	Age error (ka)
1-6	1.8631	0.2049		1.3625	0.0463	1.3025	0.0170	371.5	90.8
7-24	1.5400	0.0253		1.1725	0.0295	1.2980	0.0124	210.6	15.8
25-30	1.2305	0.0146		0.4958	0.0278	1.1960	0.0127	57.4	4.3

3757A	U (ppm)	Th (ppb)	U/Th	$^{230}Th/^{238}U$	$^{230}Th/^{238}U$ error	$^{234}U/^{238}U$	$^{234}U/^{238}U$ error	Age (ka)	Age error (ka)
1	4.32	2.1	2085	0.8621	0.0319	1.1330	0.0244	148.9	13.7
2	3.79	1.4	2787	0.8072	0.0381	1.0918	0.0344	142.1	17.0
3	2.99	1.3	2269	0.8044	0.0361	1.1119	0.0216	135.4	13.1
4	3.77	1.4	2627	0.8582	0.0354	1.1317	0.0196	147.9	13.9
5	2.95	0.8	3674	0.8677	0.0354	1.1488	0.0480	146.0	18.6
6	4.24	1.5	2851	0.9103	0.0327	1.1476	0.0177	161.9	14.3
7	0.75	0.4	1901	0.6797	0.0515	1.1091	0.0396	101.3	14.0
8	5.51	1.5	3636	0.9280	0.0358	1.1573	0.0269	165.3	17.4
9	3.79	1.0	3800	0.9549	0.0364	1.1737	0.0162	169.9	16.0
10	2.35	2.4	971	0.8680	0.0591	1.1388	0.0358	149.1	23.7
11	1.52	0.9	1628	0.7889	0.0497	1.1442	0.0251	122.9	14.9
12	3.78	1.0	3774	0.9188	0.0330	1.1648	0.0198	159.1	14.0
13	4.05	1.8	2272	0.8924	0.0350	1.1538	0.0225	153.1	14.5
14	5.09	2.3	2258	0.9026	0.0363	1.1332	0.0193	164.2	16.4
AVERAGE VALUES									
	initial $^{234}U/^{238}U$	$^{234}U/^{238}Ui$ Error		$^{230}Th/^{238}U$	$^{230}Th/^{238}U$ error	$^{234}U/^{238}U$	$^{234}U/^{238}U$ error	Age (ka)	Age error (ka)
1-14	1.2173	0.0154		0.8796	0.0205	1.1413	0.0110	152.5	8.2

3757B	U (ppm)	Th (ppb)	U/Th	$^{230}Th/^{238}U$	$^{230}Th/^{238}U$ error	$^{234}U/^{238}U$	$^{234}U/^{238}U$ error	Age (ka)	Age error (ka)
1	5.79	14.0	414	1.0870	0.0353	1.1667	0.0191	247.1	32.7
2	5.59	1.5	3648	1.0879	0.0254	1.1557	0.0189	258.5	29.6
3	5.74	1.8	3173	1.0827	0.0274	1.1517	0.0161	258.0	29.3
4	4.19	1.1	3881	1.0621	0.0281	1.1758	0.0204	222.5	22.7
5	4.14	1.0	3942	1.1373	0.0300	1.2053	0.0247	251.8	32.0
6	3.88	1.5	2602	1.1097	0.0340	1.2298	0.0228	216.0	23.3
7	3.12	1.3	2831	1.0606	0.0369	1.2308	0.0184	190.9	18.6
8	3.15	1.6	2020	1.0495	0.0419	1.2076	0.0307	196.8	25.6
9	2.58	1.0	2561	1.0282	0.0431	1.2062	0.0213	187.6	21.7
10	2.80	3.2	885	1.0274	0.0572	1.2187	0.0421	181.7	29.9
11	4.10	7.7	530	1.1303	0.0430	1.1651	0.0179	289.5	54.4
12	4.22	1.8	2336	1.1755	0.0398	1.2270	0.0200	262.2	37.7
13	3.61	1.7	2105	1.1235	0.0310	1.2242	0.0219	227.7	24.3
14	2.82	1.5	1938	1.1568	0.0533	1.2177	0.0301	255.9	50.2
15	4.36	2.4	1842	1.1457	0.0297	1.2267	0.0255	240.2	28.3
16	2.94	3.4	860	0.9907	0.0394	1.1905	0.0249	177.9	19.7
17	3.08	3.2	958	0.8919	0.0392	1.1405	0.0249	157.3	17.1
18	1.08	28.7	38	0.8778	0.0641	1.1605	0.0410	146.0	24.6
19	3.27	2.8	1187	1.0132	0.0331	1.2038	0.0226	182.0	17.2
20	0.91	3.2	285	0.7754	0.0602	1.1637	0.0326	115.3	16.6
AVERAGE VALUES									
	initial $^{234}U/^{238}U$	$^{234}U/^{238}Ui$ Error		$^{230}Th/^{238}U$	$^{230}Th/^{238}U$ error	$^{234}U/^{238}U$	$^{234}U/^{238}U$ error	Age (ka)	Age error (ka)
1-20	1.3568	0.0186		1.0744	0.0233	1.1923	0.0102	219.0	15.5
1-15	1.3774	0.0210		1.1001	0.0241	1.1956	0.0105	233.0	18.0
16-20	1.2780	0.0213		0.9398	0.0273	1.1754	0.0151	163.3	11.7

3757C	U (ppm)	Th (ppb)	U/Th	$^{230}Th/^{238}U$	$^{230}Th/^{238}U$ error	$^{234}U/^{238}U$	$^{234}U/^{238}U$ error	Age (ka)	Age error (ka)
1	3.44	3.0	1130	1.3484	0.0361	1.2342	0.0199	leaching	
2	3.86	1.8	2086	1.2763	0.0526	1.2060	0.0205	507.9	368.5
3	4.63	1.3	3498	1.1594	0.0397	1.2312	0.0209	246.2	33.0
4	3.50	1.6	2212	1.1546	0.0363	1.2326	0.0244	241.8	31.3
5	2.83	2.5	1112	1.1506	0.0414	1.2191	0.0340	249.9	42.6
6	2.79	3.2	872	1.1245	0.0529	1.2298	0.0243	224.5	35.3
7	2.67	2.9	921	1.0918	0.0438	1.2020	0.0315	223.1	34.1
8	2.40	1.8	1301	1.0997	0.0329	1.1832	0.0295	242.5	34.7
9	2.60	3.4	766	1.1413	0.1722	1.2079	0.0617	252.7	144.8
10	1.96	4.1	479	1.0576	0.0550	1.3446	0.1984	151.3	52.9
AVERAGE VALUES									
	initial $^{234}U/^{238}U$	$^{234}U/^{238}Ui$ Error		$^{230}Th/^{238}U$	$^{230}Th/^{238}U$ error	$^{234}U/^{238}U$	$^{234}U/^{238}U$ error	Age (ka)	Age error (ka)
1-10	1.4754	0.0405		1.1809	0.0317	1.2182	0.0132	275.8	32.9
3-9	1.4289	0.0324		1.1355	0.0341	1.2178	0.0151	240.1	26.3

3758	U (ppm)	Th (ppb)	U/Th	$^{230}Th/^{238}U$	$^{230}Th/^{238}U$ error	$^{234}U/^{238}U$	$^{234}U/^{238}U$ error	Age (ka)	Age error (ka)
1	6.44	5.7	1134	0.9247	0.0280	1.1435	0.0134	169.3	12.9
2	6.75	0.7	9253	0.9274	0.0254	1.1409	0.0267	171.4	15.4
3	6.35	0.6	11380	0.9259	0.0297	1.1465	0.0247	168.6	15.7
4	5.99	0.1	80040	0.8959	0.0257	1.1275	0.0176	163.6	12.4
5	6.05	-0.3	-17945	0.9008	0.0294	1.1501	0.0139	157.4	12.0
6	5.72	0.0	343113	0.9128	0.0276	1.1505	0.0169	161.8	12.3
7	5.66	-0.4	-14524	0.8966	0.0293	1.1409	0.0211	159.0	13.5
8	5.48	0.5	11876	0.9169	0.0287	1.1460	0.0243	165.1	14.7
9	5.88	-0.1	-73613	0.9103	0.0241	1.1430	0.0142	163.6	11.0
10	5.79	0.3	19177	0.8805	0.0238	1.1259	0.0152	158.1	10.7
11	5.84	-0.3	-22630	0.8851	0.0246	1.1345	0.0153	156.8	10.7
12	4.68	0.8	5952	0.8987	0.0306	1.1328	0.0201	162.7	14.4
13	6.12	0.2	28012	0.9010	0.0294	1.1610	0.0156	153.8	11.7
14	5.74	1.1	5248	0.9068	0.0322	1.1647	0.0127	154.7	12.3
15	5.61	3.1	1822	0.8758	0.0208	1.1349	0.0166	153.2	9.4
AVERAGE VALUES									
	initial $^{234}U/^{238}U$	$^{234}U/^{238}Ui$ Error		$^{230}Th/^{238}U$	$^{230}Th/^{238}U$ error	$^{234}U/^{238}U$	$^{234}U/^{238}U$ error	Age (ka)	Age error (ka)
1-15	1.2255	0.0139		0.9048	0.0196	1.1430	0.0096	161.4	8.4

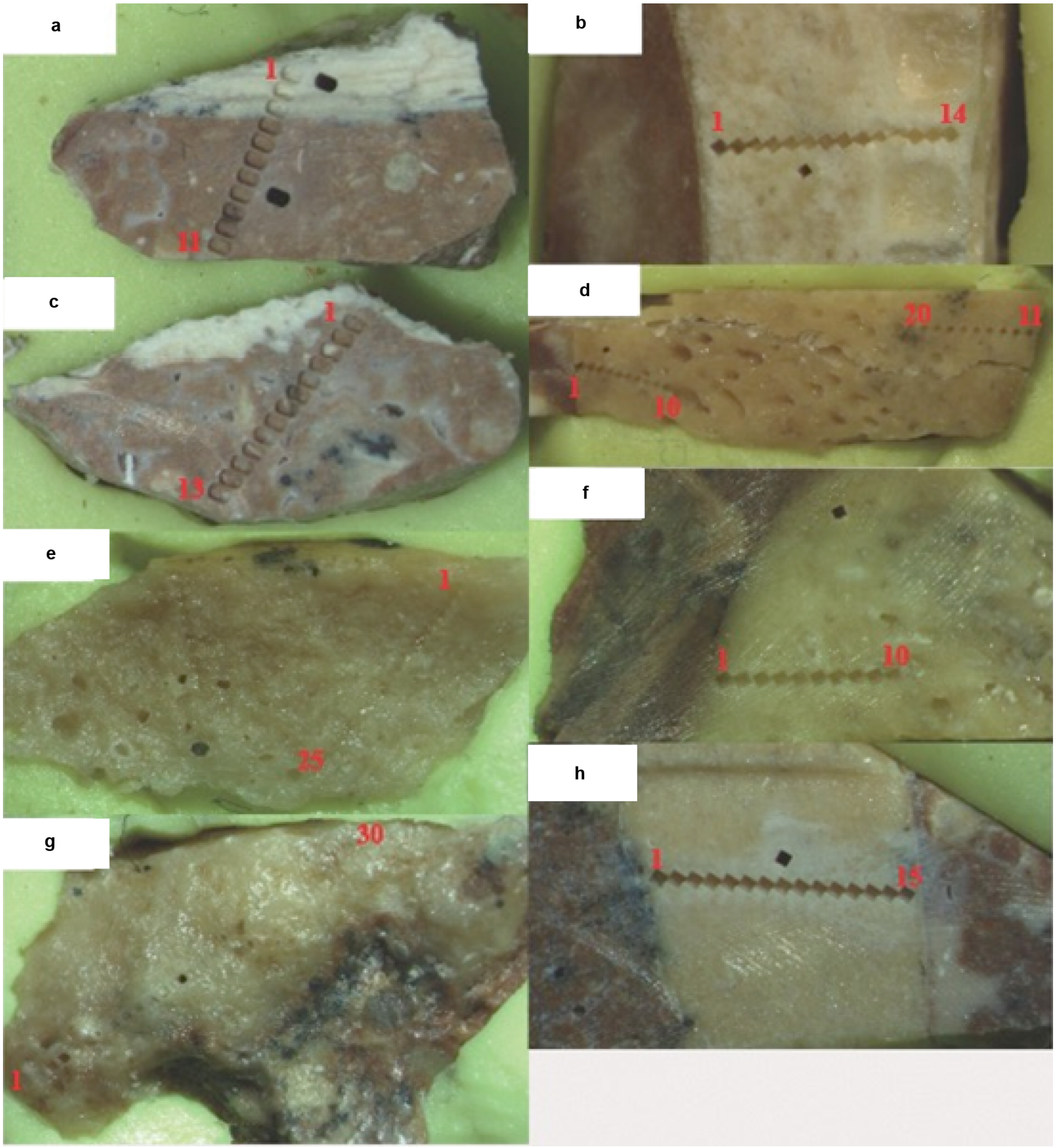

Supplementary Figure 1: Position of laser spots for U-series analyses: a, c, Breccia samples with remains of Apidima 2. **e, g,** Small sections of Apidima 1. **b, d, f, h,** Bone cross sections embedded in the breccia.

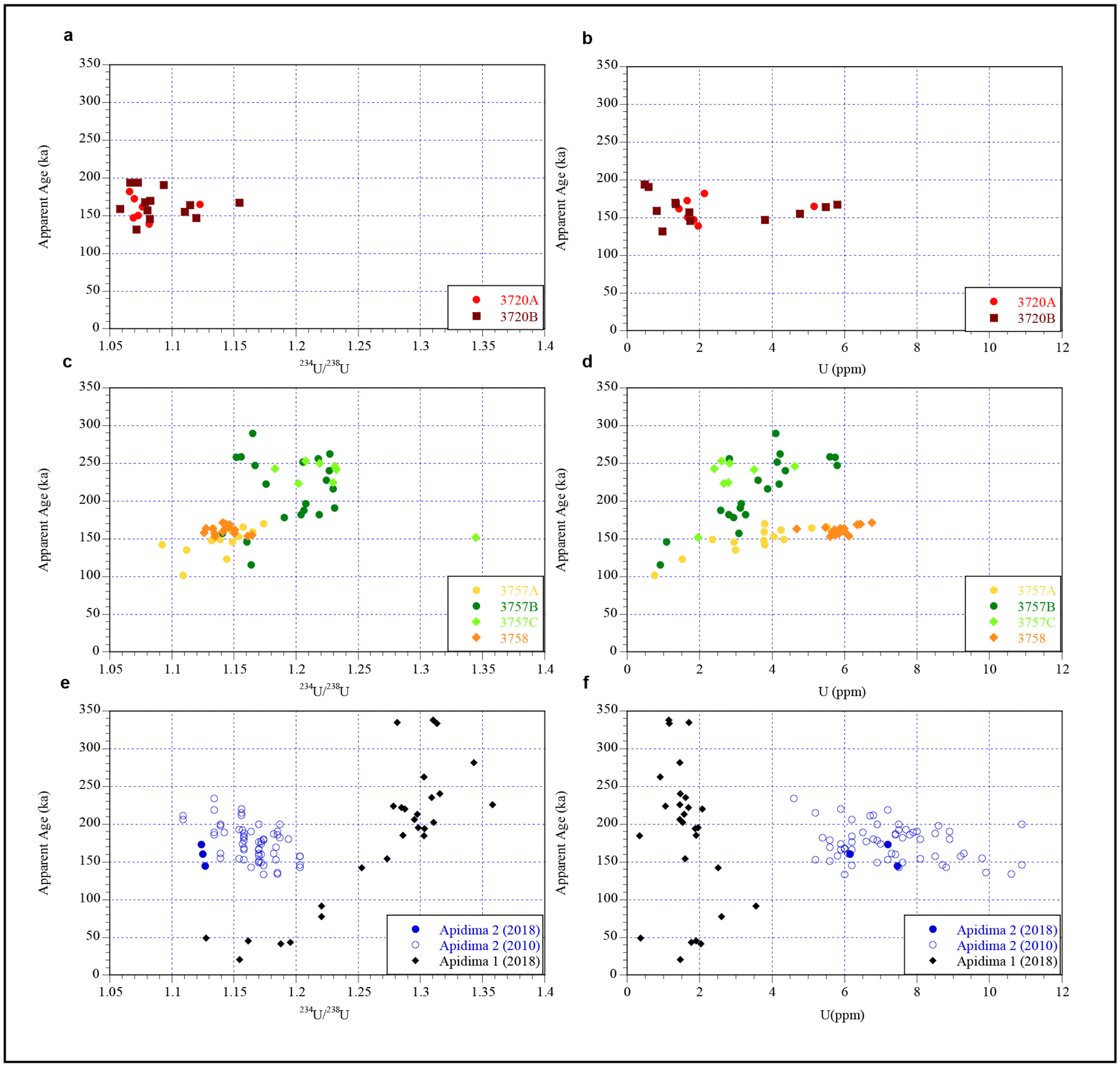

Supplementary Figure 2: Results of U-series analyses. a, c, e, measured $^{234}U/^{238}U$ ratios vs age. **b, d, f**, U-concentration vs age for breccia (A, B), faunal bones (C, D) and hominin samples (E, F).

2. Overall morphology and linear measurements of the Apidima crania

Apidima 2

Apidima 2 (Fig 1a-c, Extended Data Fig. 2) is the more complete and better known of the Apidima specimens. It preserves an almost complete face and most of the vault, but lacks the occipital bone and most of the cranial base and shows taphonomic distortions. Most of the temporal bone on the left side, and part of the right temporal squama, as well as the greater wings of the sphenoid on either side, are present, while the parietals are nearly complete but laterally fragmented. The thickness of its cranial bones (at bregma = 8 mm; at lambda = 8.3 mm), falling near the upper limit and close to the mean of the adult Neanderthal ranges, respectively [52,53], its well-developed supraorbital torus (thickness at mid orbit = 11.9 mm, within the Neanderthal range [10]), and its overall dimensions indicate that Apidima 2 is adult.

Apidima 1

Apidima 1 (Fig. 1d-f) preserves most of the left parietal and temporal bones, part of the left occipitomastoid region, broken anteriorly and inferiorly; the posterior part of the left temporal squama; a fragment of the right parietal along the sagittal suture; and a large portion of the occipital, mainly on the left. A large stone is attached to it anteriorly on the left. It is probably also adult: its bone thickness (at inion = 9.3 mm; at lambda = 7.9 mm) is well within the reported adult Neanderthal ranges [53,54]. In its linear measurements (Supplementary Table 3), the Apidima 1 specimen falls mainly in the region of overlap among taxa. However its maximum cranial breadth is relatively small, overlapping only with our *H. sapiens* sample. Its bi-auricular breadth overlaps with the ranges of all comparative samples except Middle Pleistocene Europeans. The height of the occipital plane (lambda-inion) is small, an ancestral feature most similar here to the Middle Pleistocene samples.

Supplementary Table 2. Linear measurements (in mm)*, Apidima 2 reconstruction

Variable name (Howells's abbreviation)[1]	Apidima 2 (reconstructed)[2]		Middle Pleistocene Eurasians	Middle Pleistocene Africans	Neanderthals	*H. sapiens*
Maximum cranial breadth (XCB)	**147.0 ± 2.65**	**Mean ± s.d.**	147.87 ± 8.52	145.35 ± 5.63	148.21 ± 6.18	140.93 ± 7.22
		Range	164.00-136.00	154.45-137.75	158.50-138.00	155.00-126.00
		N	7	7	12	34
Maximum frontal breadth (XFB)	**124.42 ± 2.49**	**Mean ± s.d.**	119.00 ± 3.04	117.43 ± 2.51	120.80 ± 5.51	119.41 ± 4.27
		Range	126.00-115.00	120.00-113.00	128.00-110.00	128.00-112.00
		N	9	7	15	27
Biauricular breadth (AUB)	**129.68 ± 4.33**	**Mean ± s.d.**	146.26 ± 6.76	136.09 ± 10.75	133.08 ± 10.58	128.13 ± 7.08
		Range	152.95-139.00	148.00-122.99	155.00-118.00	139.00-113.00
		N	4	6	13	29
Nasion-prosthion height (NPH)	**82.07 ± 0.93**	**Mean ± s.d.**	89.50 ± 6.36	84.97 ± 8.63	85.32 ± 5.86	69.28 ± 6.21
		Range	94.00-85.00	90.00-75.00	94.00-75.20	79.00-58.00
		N	2	3	10	27
Nasal height (NLH)	**65.70 ± 1.52**	**Mean ± s.d.**	57.33 ± 8.15	53.73 ± 8.21	62.05 ± 2.83	51.32 ± 3.90
		Range	65.50-49.20	62.00-43.50	68.50-58.00	60.20-42.70
		N	3	4	10	26
Orbit height (OBH)	**38.91 ± 0.77**	**Mean ± s.d.**	34.75 ± 1.26	36.75 ± 2.36	36.54 ± 1.07	31.41 ± 2.30
		Range	36.00-33.00	38.50-33.50	38.00-34.00	36.00-27.00
		N	4	4	11	29
Orbit breadth (OBB)	**49.68 ± 1.81**	**Mean ± s.d.**	43.62 ± 3.40	46.20 ± 2.48	44.07 ± 2.19	41.62 ± 2.72
		Range	48.00-39.40	48.50-43.30	47.00-39.50	47.00-37.00
		N	5	4	11	28
Nasal breadth (NLB)	**39.60 ± 1.13**	**Mean ± s.d.**	36.17 ± 2.25	33.52 ± 5.48	32.31 ± 3.34	26.57 ± 2.99
		Range	38.50-34.00	42.50-28.00	38.50-27.50	32.00-21.40
		N	3	5	10	26
External palate breadth (MAB)	**71.31 ± 1.57**	**Mean ± s.d.**	79.67 ± 7.23	78.25 ± 2.82	74.48 ± 4.97	65.62 ± 4.85
		Range	88.00-75.00	82.00-75.20	81.50-64.00	75.50-54.70
		N	3	4	12	26
Bimaxillary breadth (ZMB)	**114.53 ± 7.25**	**Mean ± s.d.**	110.60 ± 12.15	116.50 ± 12.01	11.54 ± 6.65	100.39 ± 6.68
		Range	119.00-93.00	130.00-107.00	120.00-100.00	114.00-88.00
		N	4	3	13	23
Zygomaxillary subtense (SSS)	**45.03 ± 0.75**	**Mean ± s.d.**	30.50 ± 6.36	32.67 ± 2.52	35,45 ± 3.86	24.34 ± 3.26
		Range	35.00-26.00	35.00-30.00	44.00-30.00	32.00-19.00
		N	2	3	11	21
Bifrontal breadth	**112.99 ± 4.16**	**Mean ± s.d.**	113.75 ± 7.89	119.25 ± 7.24	114.16 ± 5.99	105.08 ± 7.00

(FMB)		**Range**	126.00-103.50	130.00-110.00	125.00-100.00	120.00-90.00
		N	6	6	18	32
Nasio-frontal subtense (NAS)	**24.67 ± 1.33**	**Mean ± s.d.**	20.00 ± 2.53	20.50 ± 4.36	23.21 ± 3.96	16.73 ± 2.79
		Range	22.00-16.00	26.00-17.00	30.00-16.00	23.00-12.00
		N	6	4	14	30
Biorbital breadth (EKB)	**111.07 ± 2.12**	**Mean ± s.d.**	111.80 ± 9.47	119.75 ± 5.56	109.50 ± 6.69	104.72 ± 7.21
		Range	125.00-100.00	128.00-116.00	118.00-95.00	126.00-92.00
		N	5	4	12	25
Interorbital breadth (DKB)	**26.22 ± 1.80**	**Mean ± s.d.**	31.40 ± 5.59	32.40 ± 3.65	28.25 ± 4.50	23.29 ± 3.33
		Range	37.00-25.00	38.00-29.00	37.00-23.00	31.00-19.00
		N	5	5	12	21
Nasion-bregma chord (FRC)	**103.38 ± 2.56**	**Mean ± s.d.**	110.43 ± 6.35	114.25 ± 4.71	112.14 ± 7.03	114.24 ± 6.99
		Range	115.00-98.00	121.00-107.00	122.00-102.00	131.00-103.00
		N	7	8	14	33
Nasio-bregma subtense (FRS)	**12.27 ± 0.85**	**Mean ± s.d.**	24.00 ± 2.65	21.25 ± 3.54	19.93 ± 2.79	26.97 ± 2.43
		Range	26.00-29.00	26.00-16.00	24.00-15.00	33.00-23.00
		N	3	8	14	32
Bregma-lambda chord (PAC)	**108.51 ± 3.19**	**Mean ± s.d.**	105.70 ± 7.20	116.71 ± 4.50	108.08 ± 3.66	120.45 ± 5.30
		Range	119.00-95.00	122.00-109.00	113.00-103.00	129.00-107.00
		N	10	7	13	33
Bregma-lambda subtense (PAS)	**18.76 ± 1.04**	**Mean ± s.d.**	16.50 ± 2.08	18.71 ± 2.63	18.00 ± 2.65	24.56 ± 3.21
		Range	19.00-14.00	23.00-15.00	23.00-13.00	33.00-19.00
		N	4	7	13	32

[1]See Howells [55].

[2]For each variable, this column presents the mean and standard deviation among the four reconstructions of Apidima 2 (see Materials and Methods).

*Data from CS and from Arsuaga et al. [22], Ascenzi et al. [56], White et al. [57], Grine et al. [58], Creveceur et al. [59], Daura et al. [60].

Supplementary Table 3. Linear measurements (in mm)*, Apidima 1 reconstruction

Variable name (Howells's abbreviation)[1]	Apidima 1		Middle Pleistocene Eurasians	Middle Pleistocene Africans	Neanderthals	*H. sapiens*
Maximum cranial breadth (XCB)	**134.85**	**Mean ± s.d.**	147.87 ± 8.52	145.35 ± 5.63	148.21 ± 6.18	140.93 ± 7.22
		Range	164.00-136.00	154.45-137.75	158.50-138.00	155.00-126.00
		N	7	7	12	34
Biauricular breadth (AUB)	**132.24**	**Mean ± s.d.**	146.26 ± 6.76	136.09 ± 10.75	133.08 ± 10.58	128.13 ± 7.08
		Range	152.95-139.00	148.00-122.99	155.00-118.00	139.00-113.00
		N	4	6	13	29
Biasteronic breadth (ASB)	**114.99**	**Mean ± s.d.**	120.26 ± 5.26	121.27 ± 4.49	120.29 ± 6.17	113.44 ± 6.85
		Range	132.00-113.50	129.00-116.43	131.00-110.00	132.00-99.70
		N	11	6	9	32
Lambda-Inion chord	**49.71**	**Mean ± s.d.**	59.68 ± 9.30	60.16 ± 3.73	60.94	61.99 ± 3.70
		Range	71.27-49.80	67.07-53.33	-	68.03-57.33
		N	5	8	20	6
Lambda-Inion arc	**53.19**	**Mean ± s.d.**	61.94 ± 8.64	63.57 ± 6.08	61.57	63.78 ± 4.01
		Range	73.36-53.00	71.56-54.86	-	68.32-57.72
		N	5	5	17	5
Lambda-Inion substense	**6.78**	**Mean ± s.d.**	8.62 ± 3.72	10.55 ± 3.25	13.56	8.15 ± 0.73
		Range	11.64-4.46	13.93-5.50	-	9.11-7.36
		N	3	5	16	4
Lambda-Inion chord / Lambda-Inion arc (%)	**93.46**	**Mean ± s.d.**	96.28 ± 2.47	94.91 ± 2.19	88.48	96.61 ± 2.87
		Range	99.92-94.00	97.21-91.81	-	99.58-92.73
		N	5	5	17	5
Lambda-Inion subtense / Lambda-Inion chord (%)	**13.64**	**Mean ± s.d.**	12.88 ± 5.00	17.31 ± 4.60	22.09	13.12 ± 1.27
		Range	16.33-7.15	22.94-10.31	-	14.69-11.63
		N	3	5	16	4

[1]see Howells [55].

*Data from CS and from Hublin [61], Wolpoff [62], Arsuaga et al. [22], Ascenzi et al. [56], Verna et al. [16], Rightmire [63]

3. Results of the classification analysis

Supplementary Table 4. Classification, Dataset 1 (Apidima 2 face). Jackknifed classification matrix, PC1-7 (70.72% of total variance). Overall jackknifed classification success: 80.65 %. Abbreviations: Neanderthals (NEA), *H. sapiens* (HS) Middle Pleistocene Africans (MPA), Middle Pleistocene Eurasians (MPE).

	MPA	MPE	NEA	HS	Total
MPA	2	1	0	0	3
MPE	1	2	0	0	3
NEA	0	2	4	0	6
HS	0	1	1	17	19
Total	3	6	5	17	31

Supplementary Table 5. Classification, Dataset 2 (Apidima 2 neurocranium). Jackknifed classification matrix, PC1-8 (90.95 % of total variance). Overall jackknifed classification success: 78.05 %. Abbreviations: Neanderthals (NEA), *H. sapiens* (HS) Middle Pleistocene Africans (MPA), Middle Pleistocene Eurasians (MPE).

	HS	**NEA**	**MPE**	**MPA**	**Total**
HS	24	1	0	0	25
NEA	1	6	1	0	8
MPE	0	2	1	0	3
MPA	1	1	2	1	5
Total	26	10	4	1	41

Supplementary Table 6. Classification, Dataset 3 (Apidima 1 neurocranium). Jackknifed classification matrix, PC1-8 (88.58 % of total variance). Overall jackknifed classification success: 89.47 %. Abbreviations: Neanderthals (NEA), *H. sapiens* (HS) Middle Pleistocene Africans (MPA), Middle Pleistocene Eurasians (MPE).

	HS	**NEA**	**MPE**	**MPA**	**Total**
HS	22	0	0	1	23
NEA	0	5	1	0	6
MPE	0	0	4	0	4
MPA	0	1	1	3	5
Total	22	6	6	4	38

Supplementary Table 7. Classification, Dataset 4 (Apidima 1 midsagittal profile).

Jackknifed classification matrix, PC1-4 (85.43 % of total variance). Overall jackknifed classification success: 70.83 %. Abbreviations: Neanderthals (NEA), *H. sapiens* (HS) Middle Pleistocene Africans (MPA), Middle Pleistocene Eurasians (MPE).

	HS	NEA	MPE	MPA	Total
HS	23	2	1	1	27
NEA	0	8	2	0	10
MPE	0	3	1	1	5
MPA	1	0	3	2	6
Total	24	13	7	4	48

Supplementary Table 8. Classification, Dataset 5 (combined Apidima 1 - Apidima 2 dataset). Jackknifed classification matrix, PC1-4 (78.24 % of total variance). Overall jackknifed classification success: 92.11 %. Abbreviations: Neanderthals (NEA), *H. sapiens* (HS) Middle Pleistocene Africans (MPA), Middle Pleistocene Eurasians (MPE).

	HS	NEA	MPE	MPA	Total
HS	22	1	0	0	23
NEA	0	6	0	0	6
MPE	0	0	4	0	4
MPA	1	1	0	3	5
Total	23	8	4	3	38

4. Specimen abbreviations

Supplementary Table 9. Specimen abbreviations used in the plots.

Specimen	Abbreviation
Aduma 3	Adm3
Amud 1	Am1
Arago	Ar
Bodo	Bd
Broken Hill	BH
Biache St. Vaast	Bst
La Chapelle-aux-Saints 1	Ch
Dali	Da
Dolni Vestonice 3	DV3
Elandsfontein	El
Eliye Springs	ES
Feldhofer	Fh
La Ferrassie 1	Fr1
Gibraltar 1	Gb1
Guattari 1	Gt
Irhoud 1	Ir1
Irhoud 2	Ir2
La Quina 5	LQ5
Omo 1	Om1
Omo 2	Om2
Nazlet Khater 2	NK
Petralona	Pt
Qafzeh 6	Qz6
Qafzeh 9	Qz9
Reilingen	Rl
Saccopastore 1	Scc
Shanidar 1	Sh1
Shanidar 5	Sh5
Skhul 5	Sk5
Sima de los Huesos 5	Sm5
Spy 1	Sp1
Spy 2	Sp2
Swanscombe	Ssc

Supplementary References

49. Grün, R., Eggins, S., Kinsley, L., Mosely, H., Sambridge, M. Laser ablation U-series analysis of fossil bones and teeth. *Palaeogeography, Palaeoclimatology, Palaeoecology* **416**, 150-167 (2014).
50. Paul, D., White, W.M., and D. L. Turcotte, D.L. Constraints on the $^{232}Th/^{238}U$ ratio (k) of the continental crust. *Geochem. Geophys. Geosyst*. **4**(12), 1102, 1-17 (2003) doi:10.1029/2002GC000497.
51. Duval, M., Aubert, M., Hellstrom, J., Grün, R. High resolution, LA-ICP-MS mapping of U and Th isotopes in an Early Pleistocene equid tooth from Fuente Nueva-3 (Orce, Andalusia, Spain). *Quaternary Geochronology* **6**, 458-467 (2011).
52. Hershkovitz, I. *et al*. Levantine cranium from Manot cave (Israel) foreshadows the first European modern humans. *Nature* **520**, 216–219 (2015).
53. Quam, R., Martinez, I. & Arsuaga, J. L. New Observations on the Human Fossils from Petit-Puymoyen (Charente). *PaleoAnthropology* **2011**, 95−105 (2011).
54. Bastir, M. *et al*. Comparative morphology and morphometric assessment of the Neandertal occipital remains from the El Sidrón site (Asturias, Spain: years 2000–2008). *J. Hum. Evol.* 58, 68−78 (2010).
55. Howells, W. W. Cranial variation in Man. A study by multivariate analysis of patterns of differences among recent human populations. *Pap. Peabody Mus. Archaeol. Ethnol. Harvard Univ.* **67**, 1−259 (1973).
56. Ascenzi, A., Mallegni, F., Manzi, G., Segre, A. G., Naldini, E. S. A re-appraisal of

Ceprano calvaria affinities with *Homo erectus*, after the new reconstruction. *J. Hum Evol.* **39**, 443−450 (2000).

57. White, T. D. *et al*. Pleistocene *Homo sapiens* from Middle Awash, Ethiopia. *Nature* **423**, 742−747 (2003).

58. Grine, F. E. *et al*. Late Pleistocene Human skull from Hofmeyr, South Africa, and Modern Human Origins. *Science* **315**, 226−229 (2007).

59. Crevecoeur, I., Rougier, H., Grine, F. & Froment, A. Modern human cranial diversity in the Late Pleistocene of Africa and Eurasia: Evidence from Nazlet Khater, Pestera cu Oase, and Hofmeyr. *Am. J. Phys. Anthropol.* **140**, 347−358 (2009).

60. Daura, J. *et al*. New Middle Pleistocene hominin cranium from Gruta de Aroeira (Portugal). *Proc. Natl. Acad. Sci. U. S. A.* **114**, 3397−3402 (2017).

61. Hublin, J. –J. Le torus occipital transverse et les structures associées. Evolution dans le genre *Homo* (1978).

62. Wolpoff, M. H. Cranial remains of Middle Pleistocene European Hominids. *J. Hum. Evol*. **9**, 339−358 (1980).

63. Rightmire, G. P. *Homo erectus* and Middle Pleistocene hominins: brain size, skull form and species recognition. *J. Hum. Evol.* **65**, 223−252 (2013).